Theor. Appl. Climatol. 86, 215–227 (2006)
DOI 10.1007/s00704-005-0216-2

Theoretical and Applied Climatology
Printed in Austria

[1] PAGASA-DOST, Weather and Flood Forecasting Blg, Diliman, Quezon City, Philippines
[2] Institute of Environmental Science and Meteorology, University of the Philippines, Diliman, Quezon City, Philippines
[3] The Abdus Salam International Centre for Theoretical Physics, Trieste, Italy
[4] Department of Geological and Atmospheric Sciences, Iowa State University, Ames, Iowa

Regional model simulation of summer rainfall over the Philippines: Effect of choice of driving fields and ocean flux schemes

R. V. Francisco[1], J. Argete[2], F. Giorgi[3], J. Pal[3], X. Bi[3], and **W. J. Gutowski[4]**

With 7 Figures

Received December 17, 2004; revised April 19, 2005; accepted June 29, 2005
Published online July 25, 2006

Summary

The latest version of the Abdus Salam International Centre for Theoretical Physics (ICTP) regional model RegCM is used to investigate summer monsoon precipitation over the Philippine archipelago and surrounding ocean waters, a region where regional climate models have not been applied before. The sensitivity of simulated precipitation to driving lateral boundary conditions (NCEP and ERA40 reanalyses) and ocean surface flux scheme (BATS and Zeng) is assessed for 5 monsoon seasons. The ability of the RegCM to simulate the spatial patterns and magnitude of monsoon precipitation is demonstrated, both in response to the prominent large scale circulations over the region and to the local forcing by the physiographical features of the Philippine islands. This provides encouraging indications concerning the development of a regional climate modeling system for the Philippine region. On the other hand, the model shows a substantial sensitivity to the analysis fields used for lateral boundary conditions as well as the ocean surface flux schemes. The use of ERA40 lateral boundary fields consistently yields greater precipitation amounts compared to the use of NCEP fields. Similarly, the BATS scheme consistently produces more precipitation compared to the Zeng scheme. As a result, different combinations of lateral boundary fields and surface ocean flux schemes provide a good simulation of precipitation amounts and spatial structure over the region. The response of simulated precipitation to using different forcing analysis fields is of the same order of magnitude as the response to using different surface flux parameterizations in the model. As a result it is difficult to unambiguously establish which of the model configurations is best performing.

1. Introduction

During the last decades regional climate models (RCMs) have been used to study climate processes over various regions of the world (Giorgi and Mearns, 1999). Most RCM studies to date have focused on continental regions, such as the United States (e.g. Giorgi et al., 1994), Europe (e.g. Jones et al., 1995), East Asia (e.g. Kato et al., 1999), South Asia (e.g. Bhaskaran et al., 1996), South America (e.g. Seth and Rojas, 2003) and Africa (Jenkins, 2002; Sun et al., 1999). Only a few studies have been carried out over archipelagoes, such as Indonesia (Aldrian et al., 2004), and in fact no RCM studies are available for the Philippines, a country characterized by extremely complex physiographical features (Fig. 1).

Situated just off the southeastern sector of the Asian continent, the largest island of the

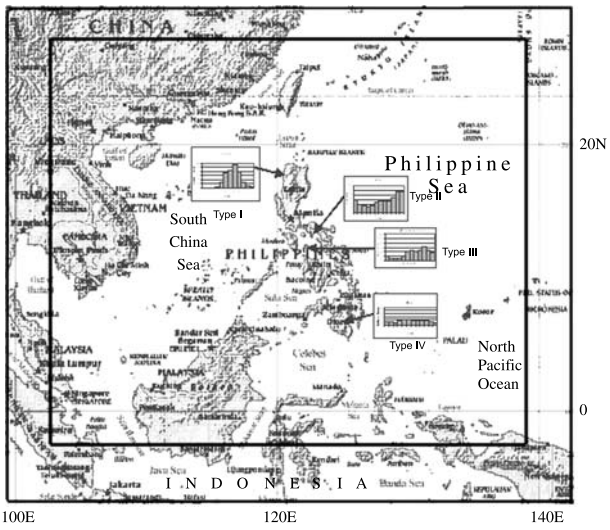

Fig. 1. Model domain (enclosed by box) with annual rainfall distributions for the four types of climate of the Philippines

Philippines, Luzon, is located in the northern part of the archipelago and is oriented from north to south with a width of about 250 km. This island has varied geographical features: the northern portion is characterized by a mountain range with a peak as high as 2700 m along the western coastal areas and a mountain range of 1400 m altitude along the eastern coasts. The two ranges are divided by the Cagayan valley. The central portion of Luzon has extensive plains, while the southern portion is volcanic with rough to hilly terrain. The second largest island, Mindanao, has mountain ranges in its northern and southern coastal areas. Consisting of approximately 7,100 islands and islets, the Philippines is surrounded by the Pacific Ocean to the east, the South China Sea to the west, the Bashi Channel to the north and the Sulu and Celebes Sea to the south. Extending from about 4.7° N to 22.5° N, the country is exposed to the influence of the inter-tropical convergence zone, tropical cyclones and subtropical anticyclones. The southwest monsoon, the northeast monsoon, the north Pacific trades and the ENSO phenomena influence the climate of the region.

The climate of the Philippines is classified by the Philippine Atmospheric, Geophysical and Astronomical Services Administration (PAGASA) according to the distribution and amount of rainfall throughout the year. Figure 1 shows the annual cycle of precipitation over four sites representative of each climate type as derived from data for the period of January 1961 to December 1990. Type I climate has 2 pronounced seasons: dry from November to April and wet during the rest of the year. These station locations have westerly exposure and are influenced by the southwest monsoon which starts in May, reaches its maximum intensity in August and retreats in October. Type II has no dry season, with pronounced rainfall from November to January. These areas have easterly exposure and are subject not only to the trades and easterlies, but also to the northeast monsoon which starts in October and lasts until March. Type III has no pronounced seasonal cycle, although it is relatively dry from November to April and wet during the rest of the year. Lastly, Type IV has rainfall more or less equally distributed throughout the year. McGregor and Nieuwulf (1998) recognize only 3 main seasons according to major airstreams: northeast monsoon, the north Pacific trades and the southwest monsoon seasons.

Because of the fine scale features of the Philippine physiography, high resolution RCMs can be especially useful tools to study climate processes over the region. On the other hand, as mentioned, the performance of these models has not been extensively tested there. Therefore, as a first step towards the development of an RCM for the Philippine region, in this paper we present an analysis of the performance and sensitivity of an RCM over a domain including the Philippine archipelago and surrounding ocean waters.

In this work we use the latest version of the Abdus Salam International Centre for Theoretical Physics (ICTP) regional model RegCM (Pal et al., 2005) and we focus on summer monsoon precipitation, which Fig. 1 shows to be high in all the different climate regimes of the region. As recommended by Giorgi and Mearns (1999), the first step in the development and testing of an RCM is to use initial and lateral driving boundary conditions from analyses of observations in the so-called ''perfect boundary condition'' mode. Such experiments allow us to identify and possibly ameliorate deficiencies in the model physics and systematic biases in the model configuration. Based on these premises, in our simulations we use analyses of observations to drive the regional model.

Current analyses of observations can be characterized by substantial errors in the tropics,

particularly in the moisture fields and over ocean areas, due to the paucity of observing data (e.g. Trenberth, 2001). This may be an important source of uncertainty in our model development effort, and therefore we test the model sensitivity to two sets of available analysis fields, those from the NCEP–NCAR reanalysis (National Center for Environmental Prediction–National Center for Atmospheric Research; Kistler et al., 2001) and those from the ECMWF ERA40 reanalysis (European Centre for Medium-range Weather Forecast; Troccoli and Kallberg, 2004).

Giorgi and Mearns (1999) point out that an RCM simulation can be also sensitive to a number of factors, such as domain size and location, resolution and choice of physical parameterizations. In terms of domain sensitivity, the study of Bhaskaran et al. (1996) indicates that over tropical Asia this may not be a dominant factor. Concerning resolution, we selected the highest affordable one capable of capturing the main physiographic features of the Philippine archipelago (see Sect. 2). Finally, the RegCM has options to use a number of different physics parameterizations (Pal et al., 2005; Giorgi et al., 1993a, b). A comprehensive assessment of the model sensitivity to these schemes is outside the purpose of this paper. Instead, we selected one physics sensitivity analysis which is of particular relevance for this region and relatively new for the RegCM, that is the model sensitivity to different surface ocean-atmosphere flux schemes.

Other details concerning the observing data used for model validation, the model configuration and the experiment design are described in the next section.

2. General description of the model and experiment design

The version of RegCM used here was originally developed by Giorgi et al. (1993a, b), but several of its components have undergone substantial changes as detailed in Pal et al. (2005). The model is hydrostatic and uses sigma vertical coordinates. Compared to the version of Giorgi et al. (1993a, b), this model version includes upgrades in the radiative transfer calculations (Giorgi et al., 1999) and in the resolvable scale precipitation calculations (Pal et al., 2000). For convective precipitation we use here the scheme of Grell (1993) with the Fritsch–Chappell closure (Fritsch and Chappell, 1980), while land surface processes are described by the Biosphere-Atmosphere Transfer Scheme (BATS). The RegCM includes a number of additional features (Pal et al., 2005) which are however less important to this study.

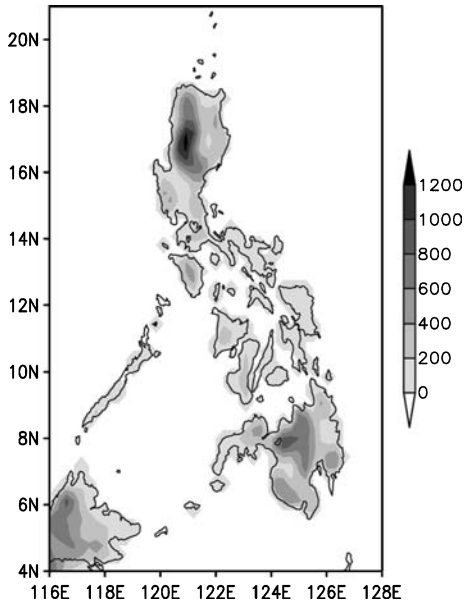

Fig. 2. Model topography over the Philippines

The RegCM uses 18 sigma levels with model top at 100 mb. The domain encompasses the inner area enclosed by the box in Fig. 1 with a horizontal grid point spacing of 30 km. The model topography over the Philippines, our region of interest, is shown in Fig. 2. At this resolution the main topographical features of the two largest islands of the Philippines are captured. Also captured are many of the islands of intermediate size. The USGS Global Land Cover Characterization (GLCC) dataset (Loveland et al., 2000) is used to generate the model land surface types. The sea surface temperatures (SST) for the experiments are from the NOAA optimum interpolation SST analysis and are produced weekly on a one-degree grid.

We focus our study on summer monsoon precipitation, which occurs from June through August, and simulate 5 monsoon seasons: 1991, 1996, 1997, 1998 and 1999. This set includes two El Niño summer conditions, 1991 and 1997; two La Niña summer conditions, 1998 and 1999, and a normal year, 1996. Each simulation starts on April 25 and ends on September 1. The first 36 days of simulation (April 25–May 31) are

however not included in the analysis to allow for model spin up.

The observational analyses used to derive initial and lateral meteorological boundary conditions are the NCEP–NCAR and the ERA40 reanalyses. The NCEP–NCAR reanalysis is a retroactive record of more than 50 years of global analyses of atmospheric fields in support of the needs of the research and climate monitoring communities (Kistler et al., 2001). It involves the recovery of land surface, ship, rawinsonde, aircraft, satellite and other data. Although the data assimilation system was kept unchanged over the reanalysis period, the reanalysis is still affected by changes in the observing system, which may cause artificial jumps and trends, particularly after the beginning of the assimilation of satellite data (Trenberth et al., 2001).

The ERA40 reanalysis is available from the Data Services of the European Centre for Medium-Range Weather Forecasts (ECMWF). It includes 6-hourly data from September 1957 to August 2002 and it also involves a comprehensive use of satellite data, starting from the early Vertical Temperature Profile Radiometer data in 1972 and later including TOVS, SSM/I, ERS and ATOVS data. The most serious problem diagnosed in the ERA40 reanalysis is excessive tropical oceanic precipitation in the later years, particularly after 1991 (Troccoli and Kallberg, 2004). The analysis is moistened over tropical oceans by the assimilation of HIRS and SSM/I data. The moistening is rejected by the assimilating model in the subsequent background forecasts, leading to higher rainfall rates over the tropical oceans than produced by the model when run either in climate-simulation mode or in the pre-satellite data assimilation mode.

2.1 Computation of ocean surface flux

One of the new features in the RegCM is the availability of two parameterizations of ocean-atmosphere exchanges of momentum, heat and moisture. Because most of our domain is covered by water, it can be expected that the simulation is sensitive to the formulation used to describe such exchanges. In the Giorgi et al. (1993a, b) version of the model, ocean-atmosphere fluxes are calculated as part of the BATS package using a standard drag coefficient formulation. The surface drag coefficient depends on the local vertical stability as measured by the bulk Richardson number, Ri_B, and on the surface roughness length, z_o, which is given a constant value of 0.0004 m.

The Richardson number Ri_B is a dimensionless measure of near surface stability and is given by

$$Ri_B = \frac{gz\Delta\theta(z)}{\theta V^2(z)} \tag{1}$$

where $\Delta\theta(z)$ is the potential temperature difference between the surface and the lowest model level at height z, g is gravity, θ is the potential temperature of the lowest model layer and $V(z)$ is the wind speed at height z.

The drag coefficient is the same for momentum, heat and moisture and is given by (Dickinson et al., 1993).

For $Ri_B < 0$:

$$C_D = C_{DN}\left(1.0 + 24.5\sqrt{-C_{DN}Ri_B}\right) \tag{2}$$

For $Ri_B \geq 0$

$$C_D = C_{DN}/(1.0 + 11.5Ri_B) \tag{3}$$

where C_{DN} is the neutral drag coefficient

$$C_{DN} = k^2/[\ln(z/z_o)]^2 \tag{4}$$

The surface fluxes of momentum, τ, latent heat, LH, and sensible heat over ocean are defined by

$$\tau = C_D V(z)\rho_a \tag{5}$$

$$SH = -\rho_a C_D V(z) C_p \Delta T$$
$$LH = -\rho_a C_D V(z)\Delta q \tag{6}$$

where ΔT and Δq are the temperature and moisture difference between the surface and the bottom model level.

In addition to the BATS scheme, the RegCM includes the ocean surface flux paramerization of Zeng et al. (1998), which also employs a drag coefficient-based bulk aerodynamic algorithm. In this case, however, the roughness length for momentum (z_o) is derived from Smith (1988) as

$$z_o = a_1\frac{\mu_*^2}{g} + a_2\frac{\nu}{\mu_*} \tag{7}$$

where ν is the kinematic viscosity of air, μ_* is the surface friction velocity, and a_1, a_2 are coefficients equal to 0.013 and 0.11, respectively.

Table 1. List of simulations performed

	Driving boundary fields	Ocean flux scheme
NCEP_Z	NCEP	Zeng
NCEP_B	NCEP	BATS
ERA40_Z	ERA40	Zeng
ERA40_B	ERA40	BATS

The roughness length for humidity (Brutsaert, 1982) is given by

$$\ln \frac{z_o}{z_{oq}} = b_1 Re_*^{1/4} + b_2 \tag{8}$$

where b_1 and b_2 are constant coefficients with values equal to 2.67 and -2.57, respectively, for wind speed in the range of 0.5–10 m s^{-1}. $Re_* = \mu_* z_o/\nu$ is the roughness Reynolds number. The roughness length for the sensible heat flux is assumed to be the same as that for the latent heat flux. For the computation of variables such as the friction velocity, μ_*, the reader is referred to Zeng et al. (1998).

The primary differences between the BATS and Zeng ocean flux schemes are that 1) in the Zeng scheme the roughness length is not constant but varies with the friction velocity and thus the state of the ocean surface; and 2) different roughness lengths are used for momentum and heat/moisture transfer. Zeng et al. (1998) showed that the introduction of the new parameterization is especially important over warm tropical oceans (such as in our experiments) where, compared to BATS, the Zeng scheme produces lower and more realistic evaporation rates.

In summary, for each of the 5 selected monsoon seasons we perform the set of four experiments reported in Table 1, which were designed to test the model sensitivity to driving analysis fields and to ocean flux scheme. This leads to a total of 20 simulations.

2.2 Observations used for model validation

Most of our analysis focuses on the simulation of precipitation. To validate the model results we use different datasets. First, we have available observing data for 40 stations of the PAGASA observing network (see Fig. 5c). Note that this network is rather sparse and most of the stations are located in low elevation areas and along the coasts of the Philippine islands. This does not provide information about the island interiors, in particular over mountainous regions. Another station-based dataset we utilize is that developed by the Climatic Research Unit (CRU) of the University of East Anglia (New et al., 2000). This consists of gridded monthly precipitation data on a 0.5° regular latitude-longitude land-only grid. Although the CRU dataset encompasses all land areas, for station-sparse regions an horizontal interpolation is performed from neighboring available stations (New et al., 2000). This implies that the CRU data over station-void mountainous regions (such as the interior of the Philippine islands) are not very reliable. A third source of observed data is the Climate Prediction Center merged analysis of precipitation (CMAP), which is an analysis of global monthly precipitation on 2.5° × 2.5° grid derived from gauge observations, satellite estimates and numerical model predictions. Although of coarse resolution, this dataset offers the advantage of providing data also over ocean areas, which comprise the largest portion of our domain. They thus provide an important tool for model validation.

3. Results and analysis

3.1 Effects of NCEP–NCAR vs. ERA40 re-analysis boundary driving fields

Figure 3a shows the precipitable water and mean moisture flux over the full model domain from the NCEP reanalysis. The data are JJA averages over the whole set of 5 simulated monsoon seasons. The moisture flow over our region mostly comes from the south. One branch of the flow, associated with the development of the East Asia monsoon, travels over the South China Sea and reaches the northern portions of the Philippines from a southwesterly direction. Conversely, the air stream that reaches the southern Philippines is directly from the south and is drier (as seen from the specific humidity field).

The NCEP and ERA40 precipitable water and moisture fluxes are compared in Fig. 3b, which shows the difference between the two reanalysis fields. It is clear that the NCEP reanalysis is characterized by generally lower levels of atmospheric specific humidity over the region. In addition, greater southerly flow is found in the ERA40 reanalysis in the southern regions of the

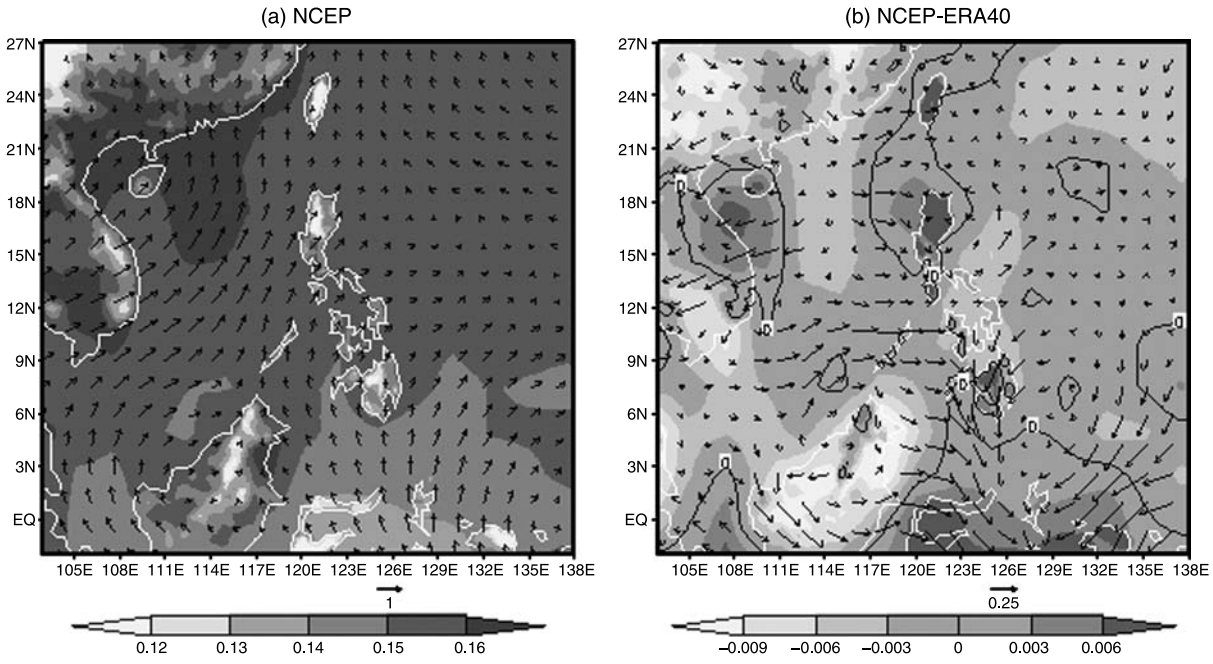

Fig. 3(a, b). Precipitable water in mm (shaded) and moisture flux in $\mathrm{kg\,m^{-2}}$ (m/s) (arrows) averaged for JJA and for the 5 simulated years for NCEP reanalysis (**a**) and difference between NCEP and ERA-40 reanalyses (**b**)

domain and greater moisture convergence over the South China Sea. All these features suggest that the ERA40 boundary fields yield conditions more favorable for precipitation in the RegCM compared to the NCEP boundary fields.

Figure 4a, c compare the 5-year average JJA precipitation over the whole domain in the NCEP_Z and ERA40_Z experiments and in the CMAP observations. In the observations two areas of intense precipitation are observed. One has a pronounced maximum west of the northern Philippines over the South China Sea and corresponds to the southwesterly monsoon moisture flow shown in Fig. 3a. The other main area of precipitation extends over the western pacific east of the Philippine archipelago and is related to the southerly moist flow over this region. Relatively dry conditions are found in the southern Philippine islands and surrounding ocean areas.

Both the NCEP_Z and ERA40_Z simulations capture the observed large scale patterns of precipitation, in particular the two wet monsoon branches and the dry conditions in the southern Philippine region. Although the patterns of precipitation are generally similar in the two sets of simulations, the precipitation amounts are consistently higher in the ERA40_Z than in the NCEP_Z experiments. This result is consistent with the moisture flow fields of Fig. 3. In particular, the NCEP_Z simulation underestimates precipitation over both the South China Sea and the western Pacific regions, while the ERA40_Z experiment reproduces well the maximum over the South China Sea but overestimates the western Pacific precipitation. Over the southern Philippine ocean areas both simulations appear to somewhat underestimate precipitation.

Table 2 reports the observed and simulated average precipitation over the interior domain as defined by the inner box of Fig. 4. Also reported is the corresponding average surface evaporation. It can be seen that precipitation is about 52% greater in the ERA40_Z than the NCEP_Z experiments and it is much closer to observations in the former. The average evaporation values in the two experiments are very close to each other, so that this difference in precipitation can be entirely attributed to the initial and boundary field forcing. Note that a similar precipitation enhancement in the ERA40 driven run compared to the NCEP driven run is found when using the BATS ocean flux scheme (experiment ERA40_B and NCEP_B).

Focusing now on the Philippine region, Fig. 5 shows the 5-year average JJA precipitation from the NCEP_Z and ERA40_Z simulations along with

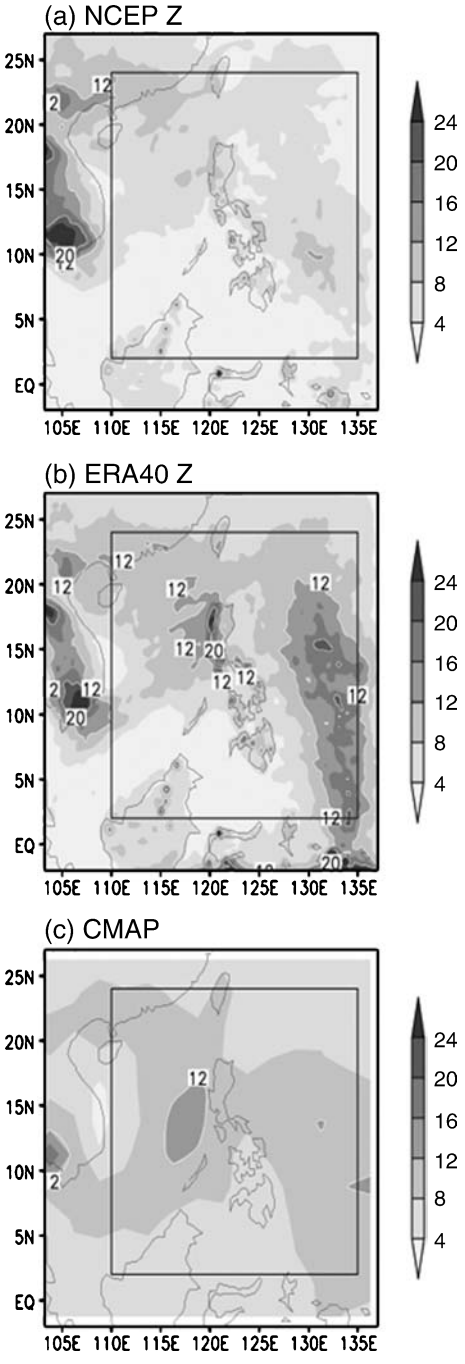

Fig. 4(a, b, c). Full domain JJA (5-year av.) precipitation in NCEP_Z, ERA40_Z and CMAP

observations from the PAGASA stations and the CRU dataset. Over the Luzon Island in the northern Philippines the model captures the strong topographically induced maximum over the western coastal regions, both when driven by the NCEP and ERA40 reanalysis fields. Between the two simulations, the precipitation amounts over this region are substantially greater in the ERA40-driven run, in excess of 10–15 mm/day. These values appear in line with the limited station data available for the western coasts of Luzon (Fig. 4c). The model also captures the secondary maxima over the eastern coastal regions of Luzon, with dry conditions in the island's interior. Note that the relatively smooth CRU data only present one maximum positioned towards the center of the Island.

Over the central and southern islands the model produces a number of localized maxima in correspondence to the local mountain features. These are difficult to validate due to the relatively coarse resolution of the observed data and to the lack of available mountain stations. The drier conditions of the southern islands, particularly Mindanao, compared to Luzon are, however, well simulated by the model.

Table 2 compares the simulated and observed 5-year average precipitation either interpolated to the station locations (when compared to the PAGASA stations) or for the entire Philippine land area (when compared to the CRU data). Precipitation in the ERA-driven runs is consistently higher than in the NCEP-driven ones, by 68% to 79% when using the Zeng scheme and by 54% to 58% when using the BATS scheme. Similarly to what is found for the full domain precipitation, although the precipitation amounts are substantially higher in the ERA-driven runs, the spatial patterns of precipitation over the Philippine islands are similar in the two sets of simulations (see Fig. 5). This is evidently because these patterns are mostly determined by the stationary forcing of topography and coastlines.

Figure 6 compares the observed and simulated interannual variability of JJA precipitation for the whole interior domain, the station location values and the Philippine gridded land area. In general, the interannual variability for the simulation years is not pronounced, both for the interior domain and the Philippine land areas, even though years with opposite El Niño phases were selected. A greater variability is found when looking at the PAGASA station values. In agreement with observations, the model also shows low interannual variability, both when using the ERA40 and the NCEP reanalyses. The variability in the model, however, is somewhat greater than in the observed datasets and a predominant consistency is found between the NCEP_Z and ERA40_Z runs when

Table 2. Simulated and observed 5-year average precipitation

	Interior domain (mm/day)		Philippines (mm/day)	
	Precipitation	Evaporation	Precipitation (gridded)	Precipitation (stations)
STN OBS				8.0
CRU			7.64	
CMAP	8.15		7.80	
NCEP_Z	5.64	4.48	5.64	5.9
NCEP_B	8.13	5.36	9.50	10.6
ERA40_Z	8.59	4.58	9.50	10.6
ERA40_B	12.48	5.73	14.62	17.0

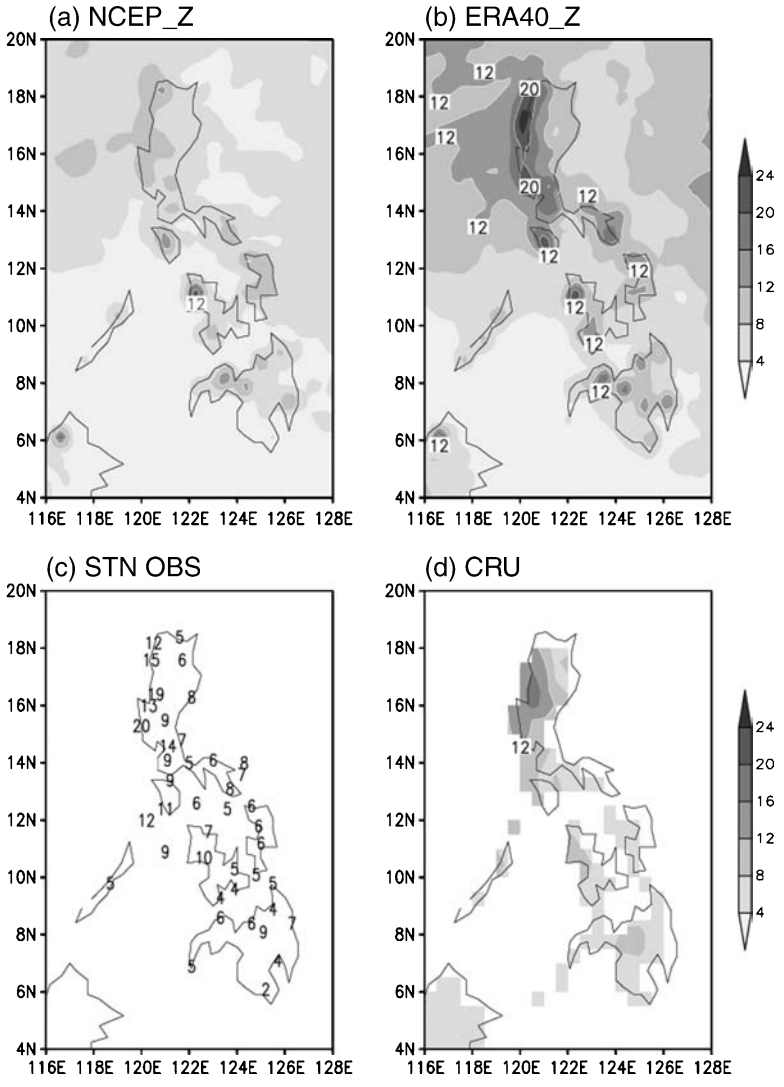

Fig. 5(a, b, c, d). Philippine JJA precipitation (5-year av) in NCEP_Z, ERA40_Z, STATIONS and CRU

looking at year-to-year variations. In most cases, consistency is found also between the simulated and observed direction of year-to-year anomalies, in particular when comparing the model results with the CRU and CMAP datasets.

3.2 BATS vs. Zeng ocean flux scheme

Figure 7a–d show the 5-year average JJA precipitation in the NCEP_B and ERA40_B experiments, both for the whole domain (Fig. 7a, b) and for the Philippine region (Fig. 7c, d). These

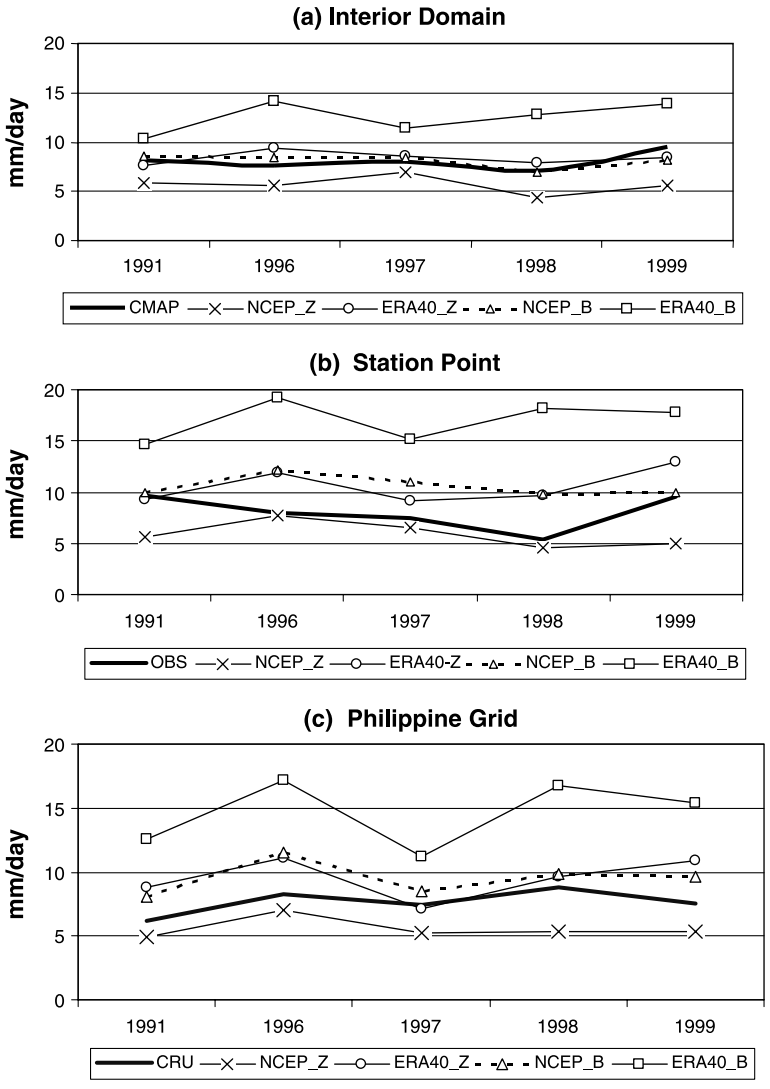

Fig. 6. Observed and simulated JJA precipitation by year averaged over: (**a**) the interior domain, (**b**) Philippine stations, and (**c**) Philippine grid

should be compared with the analogous runs using the Zeng ocean flux scheme shown in Figs. 4 and 5, respectively. From this comparison it is evident that the spatial fields of precipitation, both over the broad domain and over the Philippine sub-domain are similar in the two sets of runs, but that the use of the BATS ocean flux formulation leads to consistently higher precipitation amounts. When averaging over the interior domain, Table 2 indicates that use of the BATS scheme leads to an increase in precipitation of about 45% in the interior domain when using both the ERA40 and NCEP driving reanalysis fields. This sensitivity is slightly lower than the precipitation sensitivity to the ERA40 vs. NCEP driving fields. For the Philippine land areas the sensitivity of BATS vs. Zeng schemes is the same as that of ERA40 vs. NCEP fields.

In order to better understand the cause of the precipitation difference induced by the BATS and Zeng schemes, Table 2 presents the 5-year JJA average surface evaporation averages over ocean surfaces in the interior domain region. The surface evaporation in the BATS runs is higher than in the Zeng runs by 0.88 mm/day (NCEP runs) and 1.15 mm/day (ERA40 runs), corresponding to increases of 20% and 25%, respectively. This increase in evaporation from the ocean areas accounts only for about 30–35% of the increase in precipitation. This implies that the model responds non-linearly to the increased moisture input from the ocean surface. Calculations of the sensible heat fluxes from the oceans revealed that these are not very different between the BATS and Zeng runs (not shown). In addition, the greatest portion of the increase in precipitation between

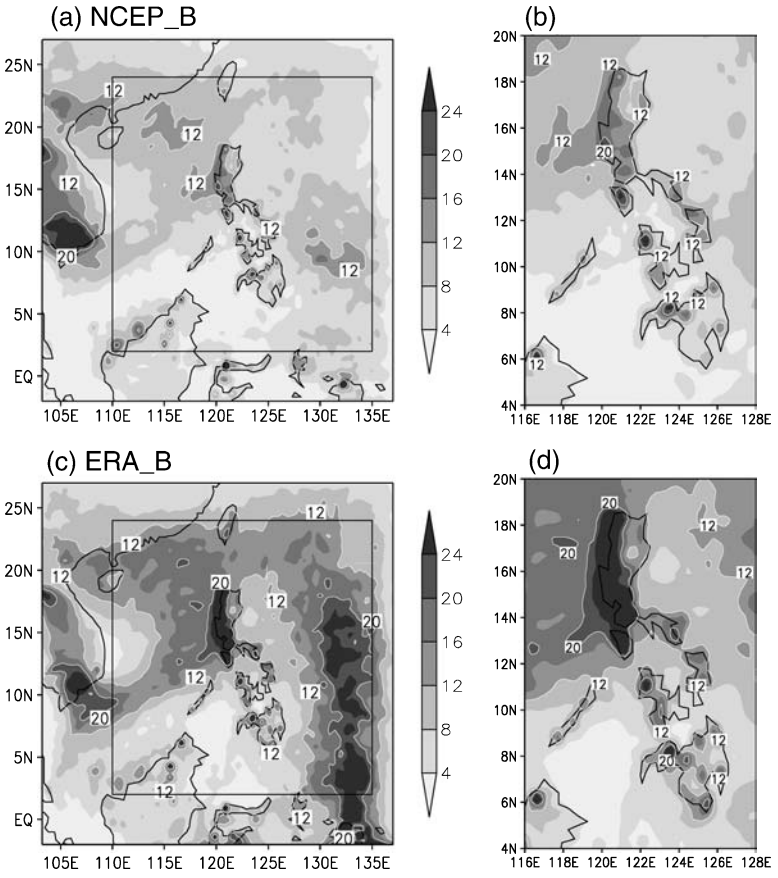

Fig. 7(a, b, c, d). JJA precipitation (5-year av.) in NCEP_B and ERA40_B for full domain and Philippines only

the two schemes occurred as non-convective precipitation. Therefore, a non-linear mechanism can be envisioned in which the additional evaporation induced by the BATS scheme increases the moisture content of the atmosphere, which leads to greater precipitation amounts and greater release of condensational heat. This in turns increases upward motions and thus further intensifies precipitation.

Our results from the comparison of the BATS and Zeng schemes are consistent with those of Zeng et al. (1998), who also found that the Zeng scheme reduced surface evaporative fluxes and precipitation over warm tropical oceans. In terms of interannual variability, Fig. 6 suggests that the BATS simulations exhibit greater interannual variations than the Zeng simulations, particularly when using the ERA40 driving fields. This, however, may just be tied to the fact that the ERA40_B configuration is characterized by the largest precipitation amount, and typically for precipitation, mean and variability are related. It should be stressed that the model response to the ocean surface scheme is amplified by the use of prescribed SST. If a coupled ocean model was used, the ocean surface would also respond to the modified evaporative flux by cooling and thus decreasing evaporation and leading to a negative feedback mechanism that would inhibit the model response.

3.3 Overall assessment of the model sensitivity to driving boundary large scale fields vs. ocean flux parameterization

Figures 4–7 and Table 2 can be used to provide an overall assessment of the model sensitivity to driving boundary large scale fields vs. choice of ocean flux parameterization. First, the BATS scheme consistently increases precipitation compared to the Zeng scheme and, similarly, the use of ERA40 driving fields consistently yields greater precipitation amounts compared to the use of NCEP driving fields. The model precipitation sensitivity to these two factors is of similar magnitude and compounds quasi-linearly when mea-

sured as percentage precipitation change. As a result, the NCEP_Z model configuration is the driest of the set, while the ERA40_B configuration is the wettest, with the NCEP_B and ERA40_Z configurations lying approximately in between and having precipitation amounts generally close to each other. Although the precipitation amounts can be quite different across the full set of experiments, the spatial structure of simulated precipitation does not change substantially, being driven by the large scale circulations over the region and by the topographic forcing of the Philippine islands.

Comparison with different observation datasets shows that precipitation is substantially overestimated in the ERA40_B and underestimated in the NCEP_Z experiments, so that, at least for our region, these two configurations do not appear to provide realistic results. Comparison with the CMAP data for the entire domain interior indicates that the NCEP_B and ERA40_Z configurations provide a good simulation of precipitation amounts and spatial structure. Over the Philippine land areas, simulated precipitation in these experiments is greater than in both the station observations and the CRU gridded dataset. However, this overestimate is likely amplified by the lack of high elevation stations both in the PAGASA dataset and in the CRU climatology. We thus hypothesize that also over the Philippine land areas the model provides a reasonable simulation of precipitation amounts.

It is difficult to assess which of the NCEP_B and ERA40_Z configuration leads to more realistic results. As mentioned, the spatial precipitation patterns over the Philippine Islands are similar in the two simulations, being mostly driven by the local topography. The large scale precipitation patterns are also generally similar in the two runs and in line with what is indicated by the CMAP observations, with the exception of an overestimate by ERA40_Z of precipitation over the western Pacific. In addition, Fig. 6 shows that the relative performance of the two model configurations varies from year to year. From the direct comparison of 5-year average fields with the CMAP data (Fig. 4), the NCEP_B run appears to provide the highest quality simulation, however the scheme of Zeng et al. (1998) is physically more advanced and realistic than the ocean flux representation in BATS.

4. Summary and conclusion

This study presents an analysis of precipitation in a set of simulations of 5 monsoon seasons over a domain covering the Philippine archipelago and surrounding oceans. The model sensitivity to driving lateral boundary conditions (NCEP and ERA40 reanalysis) and ocean surface flux scheme (BATS and Zeng) has been assessed. Overall, the model shows a good performance in simulating the spatial patterns and the magnitude of monsoon precipitation over this region, in response to both the prominent large scale circulations over the region and the local forcing by the physiographical features of the Philippine islands. This provides encouraging indications concerning the development of a regional climate modeling system for the Philippines.

On the other hand, the model shows substantial sensitivity to the forcing boundary analysis fields as well as the ocean surface flux scheme, with different combinations of these factors providing good matches to observations. This has important implications concerning the choice of model configuration for use in climate studies. In this regard the sensitivity to the ocean flux scheme is not critical, since a scheme can be chosen based on its physical soundness and comprehensiveness.

The model sensitivity to boundary reanalysis fields is however more troublesome. As already discussed, perfect boundary condition experiments are routinely used to evaluate the performance of RCMs. These experiments rely on the assumption that the forcing boundary fields provide a good representation of the large scale circulations, temperature and moisture over the region of interest. We have seen in this paper that the NCEP and ERA40 reanalyses provide markedly different descriptions of moisture amounts and fluxes over southeast Asia, and this has profound effects on the model simulation of precipitation. This disparity between ERA40 and NCEP fields is likely due to the paucity of observing data over this region, which implies that the analyzed fields rely more on the models used to produce the analysis rather than the

assimilation of observations. Because of the paucity of observations, it is also difficult to ascertain which of the two analyses is of better quality over the region.

In our experiments, the effect of using different boundary analysis fields is of the same order of magnitude as that of using different surface flux parameterizations in the model. This adds an element of ambiguity in the assessment of the best performing model configuration, since errors in the simulations are not only due to the internal model physics, but also to uncertainties in the boundary fields. The similarity of the performance by the NCEP_B and ERA40_Z experiments is a typical example of such ambiguity. Without additional information, it would be essentially impossible to claim that one surface flux scheme is better performing than the other. Such situation is likely common in tropical regions, where observations are less densely available than in mid-latitude continental regions. This adds a strong element of uncertainty in the development and evaluation of RCMs over tropical regions.

Acknowledgments

Deep appreciation goes to the Associateship Program of the Abdus Salam International Centre for Theoretical Physics for the funding support of the first and second authors' visit to the Centre. Partial financial support was also provided by the Grants-in-Aid program of the Philippine Council for Advanced Science and Technology Research Development, Department of Science and Technology, Philippines.

References

Aldrian E, Dumenil-Gates L, Jacob D, Podzum R, Gunawan D (2004) Long-term simulation of Indonesian rainfall with the MPI regional model. Clim Dyn 22: 795–814

Bhaskaran B, Jones RG, Murphy JM, Noguer M (1996) Simulations of the Indian summer monsoon using a nested regional climate model: domain size experiments. Clim Dyn 12: 573–587

Dickinson R, Henderson-Sellers A, Kennedy P (1993) Biosphere-atmosphere transfer scheme (BATS) version 1e as coupled to the NCAR community climate model, Tech. report, National Center for Atmospheric Research

Fritsch JM, Chappell CF (1980) Numerical prediction of convectively driven mesoscale pressure systems. Part I: convective parameterization. JAS 37: 1722–1733

Giorgi F, Marinucci MR, Bates GT (1993a) Development of a second-generation regional climate model (RegCM2). Part 1: Boundary layer and radiative transfer processes. Mon Wea Rev 121: 2795–2813

Giorgi F, Marinucci MR, Bates GT, deCanio G (1993b) Development of a second-generation regional climate model (RegCM2). Part II: Convective processes and assimilation of lateral boundary conditions. Mon Wea Rev 121: 2814–2832

Giorgi F, Shields Brodeur C, Bates GT (1994) Regional climate change scenarios over the United States produced with a nested regional climate model. J Climate 7(3): 375–399

Giorgi F, Mearns LO (1999) Introduction to special section: regional climate modeling revisited. J Geophys Res 104(D6): 6335–6352

Grell GA (1993) Prognostic evaluation of assumptions used by cumulus parameterizations. Mon Wea Rev 121: 754–787

Jenkins GS, Kamga A, Garba A, Diedhiou A, Morris V, Everette J (2002) Investigating the West African climate system using global/regional climate models. BAMS 83: 583–595

Jones RG, Murphy JM, Noguer M (1995) Simulation of climate-change over europe using a nested regional-climate model. 1. Assessment of control climate, including sensitivity to location of lateral boundaries. QJRM 121(526): 1415–1449

Kato H, Hirakuchi H, Nishizawa K, Giorgi F (1999) Performance of NCAR RegCM in the simulation of June and January climates over eastern Asia and the high-resolution effect of the model. J Geophys Res 104: 6455–6476

Kistler R, Kalnay E, Collins W, Saha S, White G, Woollen J, Chelliah M, Ebisuzaki W, Kanamitsu M, Kousky V, vanden Dool H, Jenne R, Viorino M (2001) The NCEP-NCAR 50-year reanalysis: monthly means CD-ROM and documentation. BAMS 82: 247–267

Loveland TR, Reed BC, Brown JF, Ohlen DO, Zhu J, Yang L, Merchant JW (2000) Development of a Global Land Cover Characteristics Database and IGBP DISCover from 1-km AVHRR Data. Int J Remote Sensing 21(6/7): 1303–1330

McGregor GR, Nieuwolt S (1998) Tropical climatology. Chichester: John Wiley

New MG, Hulme M, Jones PD (2000) Representing twentieth-century space-time climate variability. Part II: Development of 1901–1996 monthly grids of terrestrial surface climate. J Climate 13: 2217–2238

Pal JS, Small EE, Eltahir EA (2000) Simulation of regional-scale water and energy budgets: representation of subgrid cloud and precipitation processes within RegCM. J Geophys Res 105: 29579–29594

Pal JS, Giorgi F, Bi X, Elguindi N, Solmon F, Gao X, Ashfaq M, Francisco R, Bell J, Diffenbaugh N, Sloan L, Steiner A, Winter J, Zakey A (2005) The ICTP RegCM3 and RegCNET: regional climate modeling for the Developing World. Bull Amer Meteor Soc (submitted)

Seth A, Rojas M (2003) Simulation and sensitivity in a nested modeling system for South America. Part I: Reanalyses boundary forcing. J Climate 16: 2437–2453

Smith SD (1988) Coefficients of sea surface wind stress, heat flux and wind profiles as a function of wind speed and temperature. J Geophys Res 93: 15467–15472

Sun LQ, Semazzi FHM, Giorgi F, et al (1999) Application of the NCAR regional climate model to eastern Africa – 1. Simulation of the short rains of 1988. J Geophys Res-Atmos 104(D6): 6529–6548

Trenberth KE, Stepaniak DP, Hurrell JW et al (2001) Quality of reanalyses in the Tropics. J Climate 14: 1499–1510

Troccoli A, Kallberg P (2004) 13. Precipitation correction in the ERA-40 reanalyses. ERA-40 Project Report Series. ECMWF, England

Wilks D (1995) Statistical methods in atmospheric sciences. An introduction. San Diego: Academic Press, 467 pp

Xie P, Arkin PA (1997) Global precipitation: A 17-yr monthly analyses based on gauge observations, satellite estimates and numerical outputs. Bull Amer Meteor Soc 78: 2539–2558

Xie P, Arkin P (1996) Analyses of global monthly precipitation using gauge observations, satellite estimates and numerical model predictions. J Climate 9: 840–858

Zeng X, Zhao M, Dickinson RE (1998) Intercomparison of bulk aerodynamic algorithms for the computation of sea surface fluxes using TOGA COARE and TAO DATA. J Climate 11: 2628–2644

Authors' addresses: Raquel V. Francisco (e-mail: raquelfrancisco2001@yahoo.com), PAGASA-DOST, Weather and Flood Forecasting Blg., Agham Rd, Diliman, Quezon City 1104, Philippines; Josefina Argete (e-mail: argetej@yahoo.com), Institute of Environmental Science and Meteorology, University of the Philippines, Diliman, Quezon City 1104, Philippines; Filippo Giorgi, Jeremy Pal, Xunqiang Bi, The Abdus Salam International Centre for Theoretical Physics, Trieste, Italy; William J. Gutowski, Department of Geological and Atmospheric Sciences, Iowa State University, Ames, Iowa.